

Communication

Obtainment of *Threo* and *Erythro* Isomers of the 6-Fluoro-3-(2,3,6,7,8,9-Hexahydronaphtho[2,3-*b*][1,4]Dioxin-2-yl)-2,3-Dihydrobenzo[*b*][1,4]Dioxine-5-Carboxamide

Valentina Straniero *, Lorenzo Suigo, Giulia Lodigiani and Ermanno Valoti

Dipartimento di Scienze Farmaceutiche, Università degli Studi di Milano, Via Luigi Mangiagalli, 25, 20133 Milano, Italy; lorenzo.suigo@unimi.it (L.S.); giulia.lodigiani@unimi.it (G.L.); ermanno.valoti@unimi.it (E.V.)

* Correspondence: valentina.straniero@unimi.it (V.S.); Tel.: +39-02-503-19361

Abstract: 2,6-difluorobenzamides have been deeply investigated as antibacterial drugs in the last few decades. Several 3-substituted-2,6-difluorobenzamides have proved their ability to interfere with the bacterial cell division cycle by inhibiting the protein FtsZ, the key player of the whole process. Recently, we developed a novel family of 1,4-tetrahydronaphthodioxane benzamides, having an ethoxy linker, which reached sub-micromolar MICs towards Gram-positive *Staphylococcus aureus* and *Bacillus subtilis*. A further investigation of their mechanism of action should require the development of a fluorescent probe, and the consequent definition of a synthetic pathway for its obtainment. In the present work, we report the obtainment of an unexpected bicyclic side product, 6-fluoro-3-(2,3,6,7,8,9-hexahydronaphtho[2,3-*b*][1,4]dioxin-2-yl)-2,3-dihydrobenzo[*b*][1,4]dioxine-5-carboxamide, coming from the substitution of one aromatic fluorine by the *in situ* formed alkoxy group, in the final opening of an epoxide intermediate. This side product was similarly achieved, in good yields, by opening the ring of both *erythro* and *threo* epoxides, and the two compounds were fully characterized using HRMS, ¹H-NMR, ¹³C-NMR, HPLC and DSC.

Keywords: 2,6-difluorobenzamide; FtsZ inhibitors; nucleophilic aromatic substitution; side product

Citation: Straniero, V.; Suigo, L.;

Lodigiani, G.; Valoti, E. Obtainment of *Threo* and *Erythro* Isomers of the 6-Fluoro-3-(2,3,6,7,8,9-Hexahydronaphtho[2,3-*b*][1,4]Dioxin-2-yl)-2,3-Dihydrobenzo[*b*][1,4]Dioxine-5-Carboxamide. *Molbank* **2023**, *2023*, x. <https://doi.org/10.3390/xxxxx>

Academic Editors: Stefano D'Errico and Annalisa Guaragna

Received: 20 December 2022

Revised: 13 January 2023

Accepted: 15 January 2023

Published: date



Copyright: © 2023 by the authors. Submitted for possible open access publication under the terms and conditions of the Creative Commons Attribution (CC BY) license (<https://creativecommons.org/licenses/by/4.0/>).

1. Introduction

The development of novel antibiotics able to modulate innovative targets represents one of the main pursued strategies to fight the worrying problem of antimicrobial resistance [1]. This phenomenon is caused by several human-related factors, such as over-prescription of antibiotics and low investments in the antibiotic resistance field [2].

With the aim of combatting this threat, one of the most exploited and promising bacterial targets is FtsZ (Filamenting temperature sensitive Z) [3], the main protein actor of the bacterial division process, the inhibition of which leads to cell filamentation and lysis [4–7]. Physiologically, GTP-dependent FtsZ polymerization represents the first step of the whole division process, leading to the formation of the Z-ring, a polymeric circular structure, at the site partition. Other division proteins then intervene, forming the mature divisome that allows cytokinesis and cellular division [8].

In the last years, a huge number of FtsZ inhibitors have been developed, belonging to different chemical classes and interacting with the protein on two different binding sites: the GTP-binding site or the Interdomain Cleft (IDC) [4,9–11].

Considering the high variety of FtsZ inhibitors, in terms of chemical structure, origin and interaction site, they are able to inhibit the FtsZ functionality through several mechanisms of actions. For instance, PC190723 (Figure 1), one of the most studied *S. aureus* and *B. subtilis* FtsZ inhibitors, is able to stabilize a high-affinity FtsZ conformation responsible for the assembly, thus exerting antimicrobial activity [12], while other derivatives can

interfere with the GTPase activity of FtsZ polymers, evoking again their antimicrobial activity [13].

Recently, our research group reported a novel class of 1,4-naphthodioxane- or 1,4-tetrahydronaphthodioxane-benzamides as strong antimicrobials [14], acting through the inhibition of FtsZ, which resulted to be more potent than other benzamides previously reported [5,15–18]. In particular, **I** and **II** (Figure 1) possess MIC values of 0.25 $\mu\text{g}/\text{mL}$ and 0.1 $\mu\text{g}/\text{mL}$ versus both Methicillin-sensitive and Methicillin-resistant *S. Aureus*, respectively. Moreover, **I** and **II** are both active vs. *B. subtilis* with MICs under 0.1 $\mu\text{g}/\text{mL}$ [14].

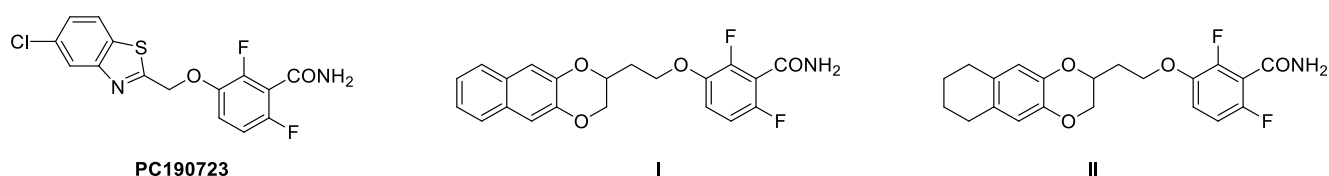


Figure 1. Structures of PC190723, derivatives **I** and **II**.

After having proved their capability to interact and inhibit both *S. aureus* and *B. subtilis* FtsZ, the need of having a fluorescent analogue (Figure 2 **Errore. L'origine riferimento non è stata trovata.**) of compound **II**, the strongest one, arose. An appropriate probe could indeed help to elucidate FtsZ inhibitors' mechanism of action, as well as to understand any possible off-target interaction, to screen for novel antibiotics, to track antibiotic uptake throughout cells and organisms, and also to detect bacterial infections. Nonetheless, despite the clear and broad utility, the number of fluorescent FZ-probes so far available [19,20] is, to the best of our knowledge, now limited to only a couple of examples.

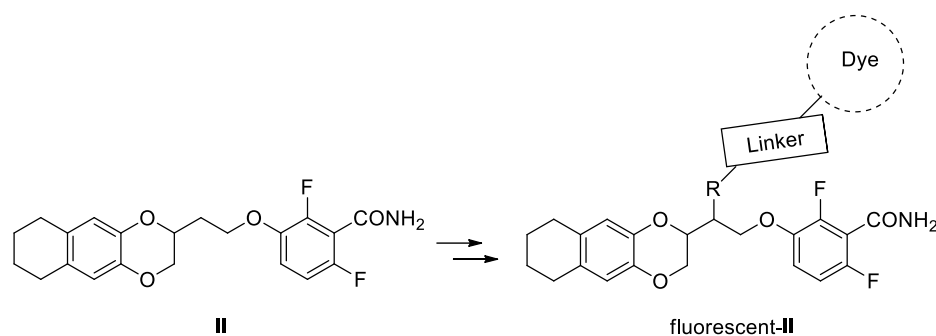
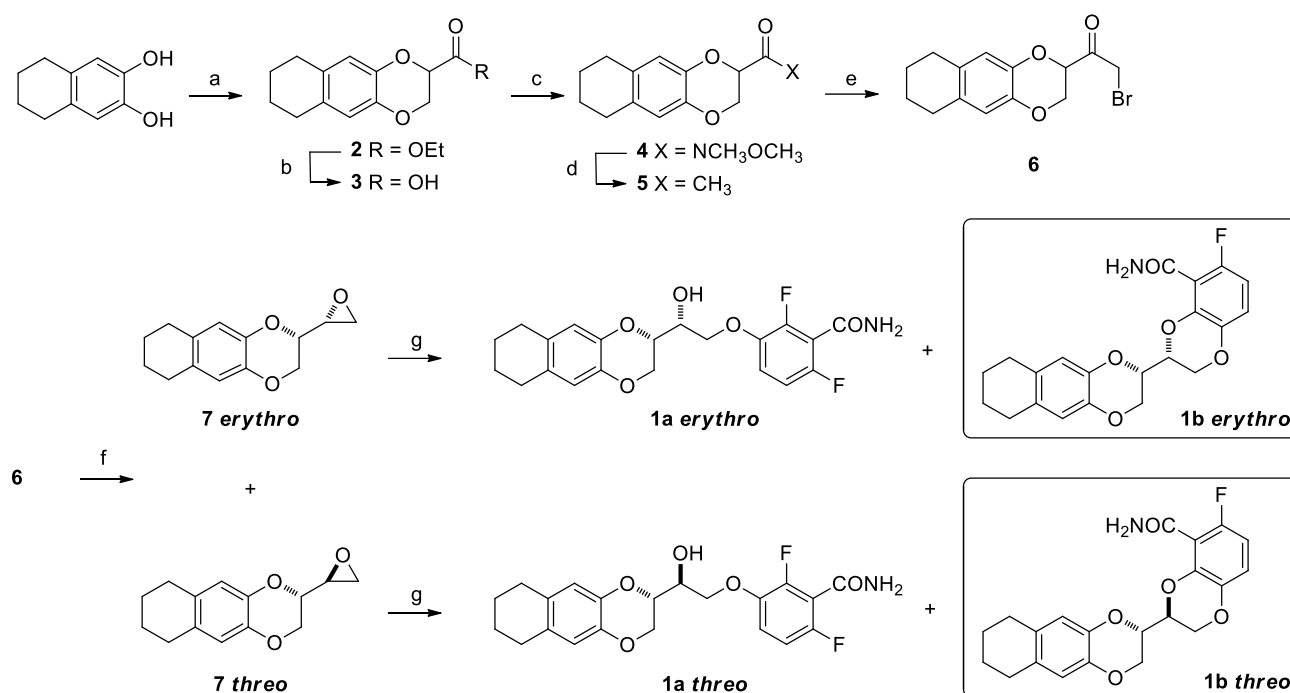


Figure 2. Structures of **II** and of the desired fluorescent analogue.

When thinking how to properly introduce a fluorescent dye, a hydroxylated analogue of **II**, compound **1a**, was designed (Scheme 1), taking inspiration from the work of Stokes and collaborators [21,22]. The introduction of the -OH was intended as a possible anchor point for the binding of a proper linker, and thus a fluorescent dye.



Scheme 1. Synthetic pathway for the obtention of both **1a** and **1b**. Reagents and conditions: (a) Ethyl 2,3-dibromopropionate, K₂CO₃, DMF, 70 °C, 1 h; (b) 10% aqueous NaOH, MeOH, RT, 30 min; (c) CDI, *N,O*-Dimethyl hydroxylamine hydrochloride, DMF, RT, 2 h; (d) CH₃MgBr, THF, RT, 1.5 h; (e) Br₂, diethyl ether, -5 °C, 3 h; (f) (I) NaBH₄, MeOH, 0–5 °C, 30 min; (II) NaH, THF, RT, 18 h; (g) 2,6-difluoro-3-hydroxybenzamide, K₂CO₃, DMF, 70 °C, 18 h.

This substituent generates a second stereocenter, and the consequent formation of both *erythro* and *threo* isomers. The obtention of **1a**, for which we followed Scheme 1, involves the final ring opening of isolated *erythro* and *threo* epoxides. In the present work, we report how both these ring openings could surprisingly allow the achievement, in significant quantities, of the bicyclic side products **1b**, the 6-fluoro-3-(2,3,6,7,8,9-hexahydronaphtho[2,3-*b*][1,4]dioxin-2-yl)-2,3-dihydrobenzo[*b*][1,4]dioxine-5-carboxamides.

We further confirmed how the obtention of these byproducts **1b erythro** and **1b threo** is favored during the epoxide opening at quite high temperatures and keeping long reaction times, which are the usual conditions adopted in the final condensation for the preparation of FtsZ inhibitors [14,17,18]. On the contrary, the formation of these side products is partially retarded, keeping milder reaction conditions.

2. Results and Discussion

The synthetic scheme developed for achieving **1a** is shown in Scheme 1 and started from the 5,6,7,8-tetrahydronaphthalene-2,3-diol, obtained as previously described [14], which was treated with freshly prepared ethyl 2,3-dibromopropionate [23], giving racemic compound **2**. The ester underwent basic hydrolysis, and the resulting carboxylic acid **3** was then converted into the Weinreb amide (**4**). Amide **4** was then quantitatively transformed into the corresponding methyl ketone **5**, by treatment with methylmagnesium bromide, similarly to what was successfully done by our research group on structurally similar derivatives [24,25].

The bromination of methyl ketone **5** was conducted with a single equivalent of bromine at low temperature, to limit the formation of polybrominated side products, and to maximize the conversion into the bromoketone **6**. Then, compound **6** underwent a tandem reaction: the first reduction of the carboxylic function with NaBH₄, achieving the instable halohydrin that was soon treated with sodium hydride, affording the two epoxides **7**, both *erythro* and *threo* isomers. The two spots of oxiranes **7** were easily distinguishable through

TLC, and the two isomers were thus isolated by flash chromatography on silica gel. Their $^1\text{H-NMR}$ spectra in CDCl_3 revealed significant differences in terms of chemical shifts and multiplicity (Figure 3).

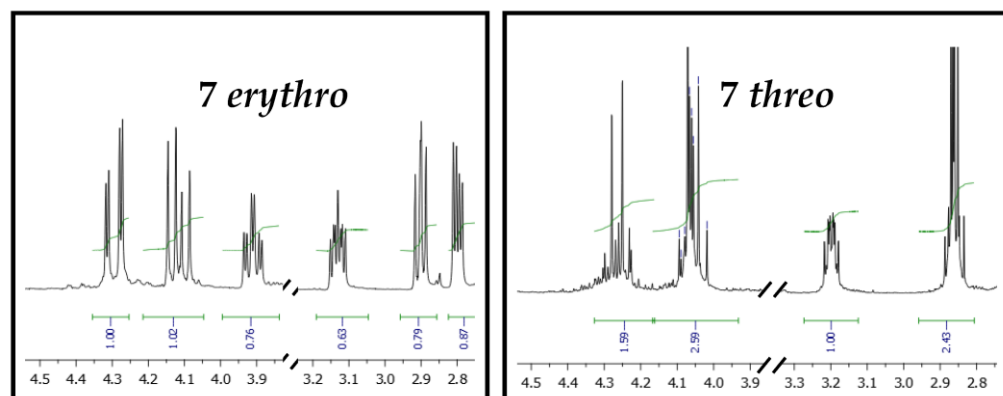


Figure 3. $^1\text{H-NMR}$ Spectra extracts of **7 erythro** and **7 threo**.

In particular, the first eluted epoxide showed six different signals, with a very clear and defined multiplicity: four doublets of doublets (two at 4.29 and 4.12 ppm, referring to the CH_2 the 1,4-dioxane portion, and two at 2.90 and 2.80 ppm, which are the two hydrogens of the epoxidic CH_2), a doublet of triplets (at 3.91 ppm, diagnostic of the hydrogen of the dioxane CH), and a double of doublets of doublets (3.13 ppm, characteristic for the epoxidic CH). The second eluted oxirane, on the contrary, showed only four multiplets: at 4.26 (1H), 4.07 (2H), 3.19 (1H) and 2.85 (2H) ppm. Moreover, the two appearances were completely different: the first eluted compound was a wax, whereas the second one was a colorless oil. The absence of any literature data on tetrahydronaphthodioxane epoxides moved us to consider the scarce and quite old data on 1,4-dioxane oxiranes [26,27].

Indeed, the peculiar NMR data of the first eluted oxirane were completely in line with what was observed by Clark and coworkers when preparing the enantiopure *erythro*-2-oxiranyl-1,4-benzodioxanes (2*R*, 1'*S*) and (2*S*, 1'*R*). Moreover, also 1,4-benzodioxane *threo* and *erythro* epoxide isomers were strongly different in terms of physic state: enantiopure *erythro* was a solid with a defined melting point (63–64 °C [27]), while the racemic one was defined as oil or with a lower melting point [26,27]. The perfect NMR overlapping, and comparable physical state difference let us define, without doubts, the diastereoisomeric identity of the two epoxides **7**.

The two **7** isomers were parallelly treated at 70 °C for 18 h in basic conditions, in the presence of 2,6-difluoro-3-hydroxybenzamide, to achieve the two final products **1a**. Unexpectedly, the TLC of the two reaction mixtures revealed the presence of two main products, different in terms of chromatographic run. In addition to the one that should refer to the desired compound **1a**, a higher spot was clearly visible in both the reactions, suggesting the formation of a more lipophilic side product.

The two reaction mixtures were worked up and the crudes purified by flash chromatography, letting the isolation, similarly in the two cases, of an undesired compound. Their $^1\text{H-NMR}$ spectra showed a surprising pattern for the aromatic signals of the benzamide. We indeed expected to observe the two doublets of triplets, which were diagnostic of the presence of two different fluorine atoms. On the contrary, both the NMR spectra revealed a triplet and a doublet of doublets, suggesting us the absence of one of the two fluorine atoms. Considering the basic reaction conditions and the prolonged reaction times, we hypothesize the formation of the two **1b** side products, in which the epoxide ring opening was soon followed by the *in situ* generation of the alcoholate, and the subsequent benzodioxane ring closure, achieving the bicyclic derivatives **1b erythro** and **1b threo**.

We further confirmed the identity of the two side products by evaluating their ^{13}C NMR spectra and their HRMS spectra. The presence of six doublets, instead of six doublets of doublets, was indeed the clear sign of the presence of a single fluorine atom. Moreover, the mass analysis confirmed the hypothesis and the elemental compositions.

We also repeated the final steps, by decreasing the reaction temperature or the reaction times, and we noticed how the side products yields were a little lower, further confirming the importance of the reaction conditions.

Finally, we also treated both **1a erythro** and **1a threo** while keeping the same reaction conditions used in the ring openings, and we noticed the formation of both **1b erythro** and **1b threo**, even with low yields.

The partial obtainment of these side products, directly from **1a erythro** and **1a threo**, suggests how these byproducts are most favored during the epoxides opening. In our opinion, the side products formation could be promoted by a concerted mechanism, in which the ring opening by the phenate is simultaneous to the cyclization due to nucleophilic substitution of the fluorine atom in phenate *ortho* position.

3. Materials and Methods

Starting materials and solvents were purchased from commercial suppliers (Merck, Darmstadt, DE, Fluorochem, Hadfield, UK, and TCI Europe N.V., Zwijndrecht, BE) and were used without further purification.

^1H and ^{13}C NMR spectra were acquired on a Varian 300 Mercury NMR spectrometer operating at 300 MHz for ^1H NMR, and 75 MHz for ^{13}C NMR; the chemical shifts are reported in ppm. Signal multiplicity is used according to the following abbreviations: s = singlet, bs = broad singlet, d = doublet, dd = doublet of doublets, ddd = doublet of doublets of doublets, td = triplet of doublets, t = triplet and m = multiplet.

Melting points were measured with a TA Q20 DSC system. TLC were performed on standard analytical silica gel layers (thickness 200 μm ; aluminum support silica gel 60 matrix with fluorescent indicator 254 nm, Sigma-Aldrich/Merck KGaA, Darmstadt, Germany). Chromatographic purifications were performed, in normal phase, using flash chromatography on Puriflash XS 420 (Sepachrom, Rho (Milan), Italy), and over different flash chromatography cartridges, filled with Merck high purity grade Silica Gel, 70–230 or 230–400 mesh particle size.

The final side products **1b erythro** and **1b threo**, as well as the benzamide derivatives **1a erythro** and **1a threo**, were analyzed by reverse-phase HPLC using a Waters XBridge C-18 column (5 μm , 4.6 mm \times 150 mm) on an Elite LaChrom HPLC system with a diode array detector (Hitachi, San Jose, CA; USA). Mobile phase: A: H_2O ; B: acetonitrile; gradient, 90% A to 10% A in 25 min with 35 min run time and a flow rate of 1 mL/min. The purity was quantified at their λ max (289 nm) and was found to be >90% for all the compounds, and the relative retention time is reported in the experimental section. High-resolution mass spectrometry (HRMS) spectra were acquired on Q-ToF SYNAPT G2-Si HDMS 8K (Waters) coupled with an electrospray ionization (ESI) source in positive (ES+) ion mode. The characterization spectra of **1b erythro** and **1b threo**, in terms of NMR (both ^1H and ^{13}C) and HRMS, is reported in the Supplementary Material.

Ethyl 2,3,6,7,8,9-hexahydronaphtho[2,3-*b*][1,4]dioxine-2-carboxylate (2): A suspension of 5,6,7,8-tetrahydronaphthalene-2,3-diol (1.50 g, 9.14 mmol) and K_2CO_3 (2.78 g, 20.1 mmol) in DMF (15 mL) was stirred at room temperature for 30 min. Ethyl 2,3-dibromopropionate (2.61 g, 10.05 mmol) was added dropwise and the reaction mixture was stirred at 70 $^\circ\text{C}$ for 1 h, the volatile solvent evaporated under vacuum, the residue diluted with ethyl acetate (20 mL), washed with 10% aqueous NaCl (5 \times 15 mL), dried with Na_2SO_4 , filtered, and concentrated under vacuum to give 1.86 g (78 %) of **2** as a yellowish oil. ^1H NMR (300 MHz, CDCl_3): δ 6.70 (s, 1H), 6.56 (s, 1H), 4.77 (t, J = 3.8 Hz, 1H), 4.34 (m, 2H), 4.27 (q, J = 7.1 Hz, 2H), 2.67 (m, 4H), 1.75 (m, 4H), and 1.29 (t, J = 7.1 Hz, 3H).

2,3,6,7,8,9-Hexahydronaphtho[2,3-*b*][1,4]dioxine-2-carboxylic acid (3): 10% aqueous NaOH (5.7 mL) was added to a solution of **2** (1.86 g, 7.09 mmol) in methanol (20 mL). The

reaction mixture was stirred for 30 min at RT, volatile solvents were evaporated, and the residue was diluted with ethyl acetate. The organic layer was washed with 10% aqueous HCl then with brine, dried over Na₂SO₄, then filtered and concentrated under vacuum to yield 1.58 g (95%) of **3** as a yellow oil. ¹H NMR (300 MHz, CDCl₃) δ 6.70 (s, 1H), 6.59 (s, 1H), 4.85 (dd, *J* = 5.1, 3.0 Hz, 1H), 4.41 (dd, *J* = 11.0, 5.1 Hz, 1H), 4.34 (dd, *J* = 11.0, 3.0 Hz, 1H), 2.66 (m, 4H), and 1.74 (m, 4H).

N-Methoxy-N-methyl-2,3,6,7,8,9-hexahydronaphtho[2,3-*b*][1,4]dioxine-2-carboxamide (4): 1,1'-Carbonyldiimidazole (1.64 g, 10.1 mmol) was added to a solution of **3** (1.58 g, 6.74 mmol) in DMF (16 mL). After stirring for 30 min, *N,O*-dimethyl hydroxylamine hydrochloride (0.99 g, 10 mmol) was added in portions, and the reaction mixture was stirred for 2 h. At completion, the DMF was evaporated, and the crude was diluted with ethyl acetate. The organic phase was washed with 10% aqueous NaHCO₃, 10% aqueous HCl and finally with brine and then dried over Na₂SO₄, filtered and concentrated under vacuum to yield 1.76 g (95%) of **4** as a brownish oil. ¹H NMR (300 MHz, CDCl₃, δ): δ 6.68 (s, 1H), 6.59 (s, 1H), 5.01 (dd, *J* = 6.7, 2.6 Hz, 1H), 4.37 (dd, *J* = 11.4, 2.6 Hz, 1H), 4.24 (dd, *J* = 11.4, 6.7 Hz, 1H), 3.78 (s, 3H), 3.26 (s, 3H), 2.66 (m, 4H), 1.74 (m, 4H).

1-(2,3,6,7,8,9-Hexahydronaphtho[2,3-*b*][1,4]dioxin-2-yl)ethanone (5): 3.0 M Methyl magnesium bromide in diethyl ether (3.2 mL) was added dropwise to a solution of **4** (1.76 g, 6.35 mmol) in dry THF (65 mL) at 0 °C under N₂. The reaction mixture was stirred at room temperature for 1.5 h and poured into a 1/1 mixture of ethyl acetate and 10% aqueous HCl (50 + 50 mL). The organic phase was then washed twice with 10% aqueous NaCl, dried over Na₂SO₄, filtered and concentrated under vacuum to yield 1.34 g (92%) of **5** as a yellowish oil. ¹H NMR (300 MHz, CDCl₃): δ 6.69 (s, 1H), 6.58 (s, 1H), 4.56 (dd, *J* = 4.9, 3.5 Hz, 1H), 4.28 (dd, *J* = 11.4, 3.5 Hz, 1H), 4.25 (dd, *J* = 11.4, 4.9 Hz, 1H), 2.68 (m, 4H), 2.29 (s, 3H), and 1.75 (m, 4H).

2-Bromo-1-(2,3,6,7,8,9-hexahydronaphtho[2,3-*b*][1,4]dioxin-2-yl)ethanone (6): Bromine (0.30 mL, 5.8 mmol) was added dropwise to a solution of **5** (1.34 g, 5.77 mmol) in diethyl ether (40 mL) at -5.0 °C. The mixture was stirred at that temperature for 3 h, washed Na₂S₂O₅ (10 mL), dried over Na₂SO₄, filtered and concentrated under vacuum, to obtain 1.80 g of **6** as a yellowish oil (quantitative yield). ¹H NMR (300 MHz, CDCl₃): δ 6.72 (s, 1H), 6.62 (s, 1H), 4.86 (dd, *J* = 4.7, 3.3 Hz, 1H), 4.40 (m, 2H), 4.33 (d, *J* = 14.0 Hz, 1H), 4.10 (d, *J* = 14.0 Hz, 1H), 2.70 (m, 4H), and 1.76 (m, 4H).

Erythro- and Threo- 2-(Oxiran-2-yl)-2,3,6,7,8,9-hexahydronaphtho[2,3-*b*][1,4]dioxine (7): NaBH₄ (0.11 g, 2.9 mmol) was added in portions to a solution of **6** (1.80 g, 5.77 mmol) in MeOH (36 mL) at 0 °C. The reaction mixture was stirred at 0 °C for 30 min, then volatile solvents were removed under vacuum. The crude was diluted with THF (15 mL) and added dropwise to a suspension of 60% NaH (0.28 g, 6.92 mmol) in THF (5 mL) at 0 °C under nitrogen atmosphere. After 30 min, the reaction mixture was warmed to RT and stirred for 18 h, then THF was evaporated, and the crude resumed with ethyl acetate (20 mL) and phosphate buffer pH = 7 (15 mL). The organic phase was washed with 10% aqueous NaCl, dried over Na₂SO₄, filtered and concentrated under vacuum to yield 1.40 g of a mixture of **7** isomers as a brown oil. Elution with 9/1 cyclohexane/ethyl acetate on silica gel gave 0.47 g of **7 erythro** (first eluted) as white wax and 0.32 g of **7 threo** (second eluted) as colorless oil (Cumulative yield of *erythro* and *threo* isomers = 59%).

7 Erythro: ¹H NMR (300 MHz, CDCl₃): δ 6.60 (s, 2H), 4.29 (dd, *J* = 11.4, 2.4 Hz, 1H), 4.12 (dd, *J* = 11.4, 6.6 Hz, 1H), 3.91 (td, *J* = 6.6, 2.4 Hz, 1H), 3.13 (ddd, *J* = 6.6, 4.1, 2.6 Hz, 1H), 2.90 (dd, *J* = 4.9, 4.1 Hz, 1H), 2.80 (dd, *J* = 4.9, 2.6 Hz, 1H), 2.67 (m, 4H), and 1.73 (m, 4H).

7 Threo: ¹H NMR (300 MHz, CDCl₃): δ 6.63 (s, 1H), 6.58 (s, 1H), 4.26 (m, 1H), 4.07 (m, 2H), 3.19 (m, 1H), 2.85 (m, 2H), 2.66 (m, 4H), and 1.74 (m, 4H).

Erythro 2,6-Difluoro-3-(2-(2,3,6,7,8,9-hexahydronaphtho[2,3-*b*][1,4]dioxin-2-yl)-2-hydroxyethoxy)benzamide (1a erythro) and erythro 6-Fluoro-3-(2,3,6,7,8,9-hexahydronaphtho[2,3-*b*][1,4]dioxin-2-yl)-2,3-dihydrobenzo[*b*][1,4]dioxine-5-carboxamide (1b erythro): A solution of 3-Hydroxy-2,6-difluorobenzamide (0.37 g, 2.1 mmol) in DMF (3

mL) was added to a solution of **7 erythro** (0.47 g, 2.0 mmol) and K_2CO_3 (0.31 g, 2.2 mmol) in DMF (2 mL) at RT. Heating and stirring at 70 °C for 18 h led to the obtainment of the side product **1b erythro** in 24% yield. DMF evaporation under vacuum, dilution with ethyl acetate (20 mL), washing with 10% aqueous NaCl (5 × 10 mL), drying over Na_2SO_4 , filtering and concentration under vacuum gave a brown residue. Elution with 6/4 to 4/6 cyclohexane/ethyl acetate on silica gel allowed the isolation of 0.32 g (Yield = 39%) of **1a erythro** and of 0.19 g (Yield = 24%) of **1b erythro** as white solids.

1a erythro: HPLC: Tr = 14.9 min. Mp = 155 °C.

1H NMR (300 MHz, d_6 -DMSO): δ 8.10 (s, 1H), 7.81 (s, 1H), 7.24 (dt, J = 9.3, 5.3 Hz, 1H), 7.04 (dt, J = 9.0, 1.8 Hz, 1H), 6.52 (s, 1H), 6.51 (s, 1H), 5.68 (d, J = 5.9 Hz, 1H), 4.32 (d, J = 9.5 Hz, 1H), 4.15 (m, 4H), 3.94 (m, 1H), 2.55 (m, 4H), and 1.64 (m, 4H)

^{13}C NMR (75 MHz, d_6 -DMSO): δ 161.8, 152.3 (dd, J = 239.3, 6.7 Hz), 148.3 (dd, J = 246.8, 8.2 Hz), 143.7 (dd, J = 10.5, 3.0 Hz), 143.3, 140.8, 129.9, 129.7, 117.0 (dd, J = 24.6, 20.3 Hz), 117.0, 116.9, 116.8, 116.7, 116.0 (dd, J = 8.5, 1.7 Hz), 111.3 (dd, J = 23.1, 3.0 Hz), 73.1, 71.4, 67.8, 64.9, 28.5, and 23.2.

1b erythro: HPLC: Tr = 15.3 min. Mp = 266 °C. HRMS (TOF ES⁺, Na⁺-adduct): m/z 408.1229, 409.1263, and 410.1289. Calculated mass 408.1218, evaluated mass 408.1229.

1H NMR (300 MHz, d_6 -DMSO): δ 7.91 (s, 1H), 7.63 (s, 1H), 6.92 (d, J = 9.0, 5.4 Hz, 1H), 6.73 (t, J = 9.0 Hz, 1H), 6.58 (s, 1H), 6.55 (s, 1H), 4.44 (dd, J = 11.6, 3.5 Hz, 1H), 4.33–4.28 (m, 4H), 4.17 (dd, J = 12.1, 6.5 Hz, 1H), 2.57 (m, 4H), and 1.64 (m, 4H).

^{13}C NMR (75 MHz, d_6 -DMSO): δ 163.4, 153.1 (d, J = 237.0 Hz), 141.1, 140.1, 139.7 (d, J = 3.0 Hz), 139.5 (d, J = 9.0 Hz), 130.24, 130.17, 117.6 (d, J = 9.0 Hz), 117.03, 117.01, 116.9 (d, J = 27.0 Hz), 108.3 (d, J = 25.5 Hz), 70.1, 70.0, 64.3, 63.6, 28.5, and 23.2.

Threo 2,6-Difluoro-3-(2-(2,3,6,7,8,9-hexahydronaphtho[2,3-*b*][1,4]dioxin-2-yl)-2-hydroxyethoxy)benzamide (1a threo) and threo 6-Fluoro-3-(2,3,6,7,8,9-hexahydronaphtho[2,3-*b*][1,4]dioxin-2-yl)-2,3-dihydrobenzo[*b*][1,4]dioxine-5-carboxamide (1b threo): **1a** and **1b threo** were obtained from **7 threo** (0.30 g, 1.3 mmol), following the same procedure of **1a erythro** and **1b erythro**, achieving 0.16 g (Yield = 31%) of **1a threo** and 80 mg (Yield = 16%) of **1b threo** as white solids.

1a threo: HPLC Tr = 14.5 min. Mp = 147 °C.

1H NMR (300 MHz, d_6 -DMSO): δ 8.09 (s, 1H), 7.81 (s, 1H), 7.27 (dt, J = 9.4, 5.3 Hz, 1H), 7.05 (dt, J = 9.0, 1.9 Hz, 1H), 6.53 (s, 1H), 6.52 (s, 1H), 5.49 (d, J = 5.8 Hz, 1H), 4.33 (dd, J = 11.2, 2.0 Hz, 1H), 4.09 (m, 5H), 2.56 (m, 4H), and 1.64 (m, 4H).

^{13}C NMR (75 MHz, d_6 -DMSO): δ 161.8, 152.3 (dd, J = 239.3, 6.7 Hz), 148.3 (dd, J = 246.8, 8.2 Hz), 143.7 (dd, J = 10.5, 3.0 Hz), 143.3, 140.8, 129.9, 129.7, 117.0 (dd, J = 24.6, 20.3 Hz), 117.0, 116.9, 116.8, 116.7, 116.0 (dd, J = 8.5, 1.7 Hz), 111.3 (dd, J = 23.1, 3.0 Hz), 73.1, 71.4, 67.8, 64.9, 28.5, and 23.2.

1b threo: HPLC Tr = 13.3 min. Mp = 290 °C with decomposition. HRMS (TOF ES⁺, Na⁺-adduct): m/z 408.1222, 409.1253, and 410.1277. Calculated mass 408.1218, evaluated mass 408.1222.

1H NMR (300 MHz, d_6 -DMSO): δ 7.75 (s, 1H), 7.56 (s, 1H), 6.91 (d, J = 8.9, 5.5 Hz, 1H), 6.71 (t, J = 8.9 Hz, 1H), 6.55 (s, 1H), 6.52 (s, 1H), 4.48–4.37 (m, 4H), 4.21 (dd, J = 11.9, 8.1 Hz, 1H), 4.08 (dd, J = 11.9, 8.3 Hz, 1H), 2.56 (m, 4H), and 1.64 (m, 4H).

^{13}C NMR (75 MHz, d_6 -DMSO): δ 163.4, 153.2 (d, J = 236.8 Hz), 141.0, 140.8 (d, J = 3.0 Hz), 140.4 (d, J = 10.1 Hz), 139.7, 130.1, 130.0, 117.61 (d, J = 9.0 Hz), 117.59, 117.5, 117.0 (d, J = 21.1 Hz), 108.2 (d, J = 22.3 Hz), 72.1, 71.7, 64.5, 64.2, 28.5, and 23.2.

Conversion of 1a erythro to 1b erythro: A solution of **1a erythro** (0.10 g, 0.25 mmol) in DMF (1 mL) was added to a suspension of K_2CO_3 (0.070 g, 0.50 mmol) in DMF (1 mL) at RT. The mixture was heated at 70 °C and stirred for 18 h, then DMF was evaporated under vacuum. The residue was diluted with ethyl acetate (10 mL), washed with 10% aqueous NaCl (5 × 5 mL), dried over Na_2SO_4 , then filtered and concentrated under vacuum, yielding a brown residue. Elution with 1/1 cyclohexane/ethyl acetate on silica gel allowed the isolation of 34 mg (35%) of **1b erythro** as a white solid.

Conversion of 1a threo to 1b threo: **1b threo** was obtained from **1a threo** (0.10 g, 0.25 mmol), following the same procedure seen for **1b erythro**, achieving 29 mg (30%) of **1b threo** as a white solid.

4. Conclusions

The two *threo* and *erythro* isomers of the 6-fluoro-3-(2,3,6,7,8,9-hexahydronaphtho[2,3-*b*][1,4]dioxin-2-yl)-2,3-dihydrobenzo[*b*][1,4]dioxine-5-carboxamide were obtained as a significant and abundant side product, when opening the two isomers of the 2-(oxiran-2-yl)-2,3,6,7,8,9-hexahydronaphtho[2,3-*b*][1,4]dioxines with a 2,6-difluorophenolate, stirring at 70 °C and keeping overnight reaction times.

The structure of these two side products was firstly hypothesized by carefully evaluating the ¹H-NMR spectra, which revealed the absence of a fluorine atom, and then confirmed by both ¹³C-NMR and HRMS spectra. The diastereoisomeric identity was defined after having characterized the isomer nature of the starting epoxides, by NMR comparison with literature enantiopure 1,4-benzodioxane oxiranes. The side products were further characterized by HPLC and DSC, fully detailing these novel and unexpected byproducts.

Supplementary Materials: The following are available online: Compound **1b erythro**; Figure S1: copy of ¹H-NMR spectrum in DMSO-*d*₆; Figure S2: copy of ¹³C-NMR spectrum in DMSO-*d*₆; Figure S3: copy of HRMS spectrum; Figure S4: copy of Elemental Composition Report; Compound **1b threo**; Figure S5: copy of ¹H-NMR spectrum in DMSO-*d*₆; Figure S6: copy of ¹³C-NMR spectrum in DMSO-*d*₆; Figure S7: copy of HRMS spectrum; and Figure S8: copy of Elemental Composition Report.

Author Contributions: Conceptualization, L.S., V.S. and E.V.; investigation, L.S. and G.L.; data curation, L.S. and V.S.; writing—original draft preparation, V.S. and L.S.; writing—review and editing, V.S. and E.V.; supervision, V.S. and E.V. All authors have read and agreed to the published version of the manuscript.

ORCID: Valentina Straniero <https://orcid.org/0000-0002-5089-0879>; Lorenzo Suigo <https://orcid.org/0000-0002-8958-1547>; Giulia Lodigiani <https://orcid.org/0000-0001-7369-7708>; Ermanno Valoti <https://orcid.org/0000-0002-5608-3875>.

Funding: This research received no external funding.

Data Availability Statement: The data presented in this study are available in the Supplementary Materials.

Acknowledgments: Mass spectrometry analyses were performed at the Mass Spectrometry facility of Unitech COSPECT at the University of Milan (Italy). The authors acknowledge the support of the APC central fund of the University of Milan.

Conflicts of Interest: The authors declare no conflict of interest.

Sample Availability: Samples of the compounds are available from the authors.

References

1. World Health Organization. Global Action Plan on Antimicrobial Resistance. 2015. <https://www.who.int/publications/i/item/9789241509763>, (accessed on 15 October 2022), ISBN 9789241509763.
2. World Health Organization. Antibiotic Resistance: Prevention and Control. Available online: <https://www.who.int/news-room/fact-sheets/detail/antibiotic-resistance#:~:text=Antibiotic%20resistance%20is%20accelerated%20by,poor%20infection%20prevention%20and%20control> (accessed on 15 October 2022).
3. Pradhan, P.; Margolin, W.; Beuria, T.K. Targeting the Achilles Heel of FtsZ: The Interdomain Cleft. *Front. Microbiol.* **2021**, *12*, 732796. <https://doi.org/10.3389/fmicb.2021.732796>.
4. Casiraghi, A.; Suigo, L.; Valoti, E.; Straniero, V. Targeting Bacterial Cell Division: A Binding Site-Centered Approach to the Most Promising Inhibitors of the Essential Protein FtsZ. *Antibiotics* **2020**, *9*, 69. <https://doi.org/10.3390/antibiotics9020069>.
5. Straniero, V.; Pallavicini, M.; Chiodini, G.; Zanotto, C.; Volontè, L.; Radaelli, A.; Bolchi, C.; Fumagalli, L.; Sanguinetti, M.; Menchinelli, G.; et al. 3-(Benzodioxan-2-ylmethoxy)-2,6-difluorobenzamides bearing hydrophobic substituents at the 7-position of the benzodioxane nucleus potently inhibit methicillin-resistant Sa and Mtb cell division. *Eur. J. Med. Chem.* **2016**, *120*, 227–243. <https://doi.org/10.1016/j.ejmech.2016.03.068>.

6. Adams, D.W.; Wu, L.J.; Czaplowski, L.G.; Errington, J. Multiple effects of benzamide antibiotics on FtsZ function. *Mol. Microbiol.* **2011**, *80*, 68–84. <https://doi.org/10.1111/j.1365-2958.2011.07559.x>.
7. Adams, D.W.; Wu, L.J.; Errington, J. A benzamide-dependent ftsZ mutant reveals residues crucial for Z-ring assembly. *Mol. Microbiol.* **2016**, *99*, 1028–1042. <https://doi.org/10.1111/mmi.13286>.
8. Haeusser, D.P.; Margolin, W. Splitsville: Structural and functional insights into the dynamic bacterial Z ring. *Nat. Rev. Microbiol.* **2016**, *14*, 305–319. <https://doi.org/10.1038/nrmicro.2016.26>.
9. Carro, L. Recent Progress in the Development of Small-Molecule FtsZ Inhibitors as Chemical Tools for the Development of Novel Antibiotics. *Antibiotics* **2019**, *8*, 217. <https://doi.org/10.3390/antibiotics8040217>.
10. Tripathy, S.; Sahu, S.K. FtsZ inhibitors as a new genera of antibacterial agents. *Bioorganic Chem.* **2019**, *91*, 103169. <https://doi.org/10.1016/j.bioorg.2019.103169>.
11. Han, H.; Wang, Z.; Li, T.; Da Teng; Mao, R.; Hao, Y.; Yang, N.; Wang, X.; Wang, J. Recent progress of bacterial FtsZ inhibitors with a focus on peptides. *FEBS J.* **2021**, *288*, 1091–1106. <https://doi.org/10.1111/febs.15489>.
12. Elsen, N.L.; Lu, J.; Parthasarathy, G.; Reid, J.C.; Sharma, S.; Soisson, S.M.; Lumb, K.J. Mechanism of action of the cell-division inhibitor PC190723: Modulation of FtsZ assembly cooperativity. *J. Am. Chem. Soc.* **2012**, *134*, 12342–12345. <https://doi.org/10.1021/ja303564a>.
13. Fang, Z.; Li, Y.; Zheng, Y.; Li, X.; Lu, Y.-J.; Yan, S.-C.; Wong, W.-L.; Chan, K.-F.; Wong, K.-Y.; Sun, N. Antibacterial activity and mechanism of action of a thiophenyl substituted pyrimidine derivative. *RSC Adv.* **2019**, *9*, 10739–10744. <https://doi.org/10.1039/C9RA01001G>.
14. Straniero, V.; Sebastián-Pérez, V.; Suigo, L.; Margolin, W.; Casiraghi, A.; Hrast, M.; Zanutto, C.; Zdovc, I.; Radaelli, A.; Valoti, E. Computational Design and Development of Benzodioxane-Benzamides as Potent Inhibitors of FtsZ by Exploring the Hydrophobic Subpocket. *Antibiotics* **2021**, *10*, 442. <https://doi.org/10.3390/antibiotics10040442>.
15. Chiodini, G.; Pallavicini, M.; Zanutto, C.; Bissa, M.; Radaelli, A.; Straniero, V.; Bolchi, C.; Fumagalli, L.; Ruggeri, P.; De Giuli Morghen, C.; et al. Benzodioxane-benzamides as new bacterial cell division inhibitors. *Eur. J. Med. Chem.* **2015**, *89*, 252–265. <https://doi.org/10.1016/j.ejmech.2014.09.100>.
16. Straniero, V.; Zanutto, C.; Straniero, L.; Casiraghi, A.; Duga, S.; Radaelli, A.; De Giuli Morghen, C.; Valoti, E. 2,6-Difluorobenzamide Inhibitors of Bacterial Cell Division Protein FtsZ: Design, Synthesis, and Structure-Activity Relationships. *ChemMedChem* **2017**, *12*, 1303–1318. <https://doi.org/10.1002/cmde.201700201>.
17. Straniero, V.; Sebastián Pérez, V.; Hrast, M.; Zanutto, C.; Casiraghi, A.; Suigo, L.; Zdovc, I.; Radaelli, A.; De Giuli Morghen, C.; Valoti, E. Benzodioxane-benzamides as antibacterial agents: Computational and SAR studies to evaluate the influence of the 7-substitution in FtsZ interaction. *ChemMedChem* **2020**, *2*, 195–209. <https://doi.org/10.1002/cmde.201900537>.
18. Straniero, V.; Suigo, L.; Casiraghi, A.; Sebastián-Pérez, V.; Hrast, M.; Zanutto, C.; Zdovc, I.; De Giuli Morghen, C.; Radaelli, A.; Valoti, E. Benzamide Derivatives Targeting the Cell Division Protein FtsZ: Modifications of the Linker and the Benzodioxane Scaffold and Their Effects on Antimicrobial Activity. *Antibiotics* **2020**, *9*, 4. <https://doi.org/10.3390/antibiotics9040160>.
19. Artola, M.; Ruíz-Avila, L.B.; Ramírez-Aportela, E.; Martínez, R.F.; Araujo-Bazán, L.; Vázquez-Villa, H.; Martín-Fontecha, M.; Oliva, M.A.; Martín-Galiano, A.J.; Chacón, P.; et al. The structural assembly switch of cell division protein FtsZ probed with fluorescent allosteric inhibitors. *Chem. Sci.* **2017**, *8*, 1525–1534. <https://doi.org/10.1039/C6SC03792E>.
20. Ferrer-González, E.; Fujita, J.; Yoshizawa, T.; Nelson, J.M.; Pilch, A.J.; Hillman, E.; Ozawa, M.; Kuroda, N.; Al-Tameemi, H.M.; Boyd, J.M.; et al. Structure-Guided Design of a Fluorescent Probe for the Visualization of FtsZ in Clinically Important Gram-Positive and Gram-Negative Bacterial Pathogens. *Sci. Rep.* **2019**, *9*, 20092. <https://doi.org/10.1038/s41598-019-56557-x>.
21. Stokes, N.R.; Baker, N.; Bennett, J.M.; Berry, J.; Collins, I.; Czaplowski, L.G.; Logan, A.; Macdonald, R.; Macleod, L.; Peasley, H.; et al. An improved small-molecule inhibitor of FtsZ with superior in vitro potency, drug-like properties, and in vivo efficacy. *Antimicrob. Agents Chemother.* **2013**, *57*, 317–325. <https://doi.org/10.1128/AAC.01580-12>.
22. Stokes, N.R.; Baker, N.; Bennett, J.M.; Chauhan, P.K.; Collins, I.; Davies, D.T.; Gavade, M.; Kumar, D.; Lancett, P.; Macdonald, R.; et al. Design, synthesis and structure-activity relationships of substituted oxazole-benzamide antibacterial inhibitors of FtsZ. *Bioorganic Med. Chem. Lett.* **2014**, *24*, 353–359. <https://doi.org/10.1016/j.bmcl.2013.11.002>.
23. Casiraghi, A.; Valoti, E.; Suigo, L.; Artasensi, A.; Sorvillo, E.; Straniero, V. How Reaction Conditions May Influence the Regioselectivity in the Synthesis of 2,3-Dihydro-1,4-benzoxathine Derivatives. *J. Org. Chem.* **2018**, *83*, 13217–13227. <https://doi.org/10.1021/acs.joc.8b02012>.
24. Suigo, L.; Lodigiani, G.; Straniero, V.; Valoti, E. (3-Methylene-2,3-dihydronaphtho[2,3-b][1,4]dioxin-2-yl)methanol. *Molbank* **2022**, *2022*, M1521. <https://doi.org/10.3390/M1521>.
25. Straniero, V.; Casiraghi, A.; Fumagalli, L.; Valoti, E. How do reaction conditions affect the enantiopure synthesis of 2-substituted-1,4-benzodioxane derivatives? *Chirality* **2018**, *30*, 943–950. <https://doi.org/10.1002/chir.22968>.
26. Clark, R.D.; Caroon, J.M.; Kluge, A.F.; Repke, D.B.; Roszkowski, A.P.; Strosberg, A.M.; Baker, S.; Bitter, S.M.; Okada, M.D. Synthesis and antihypertensive activity of 4'-substituted spiro4H-3,1-benzoxazine-4,4'-piperidin-2(1H)-ones. *J. Med. Chem.* **1983**, *26*, 657–661. <https://doi.org/10.1021/jm00359a007>.
27. Clark, R.D.; Kurz, L.J. Synthesis of the Enantiomers of Erythro-2-oxiranyl-1,4-benzodioxan. *Heterocycles* **1985**, *23*, 2005. <https://doi.org/10.3987/R-1985-08-2005>.